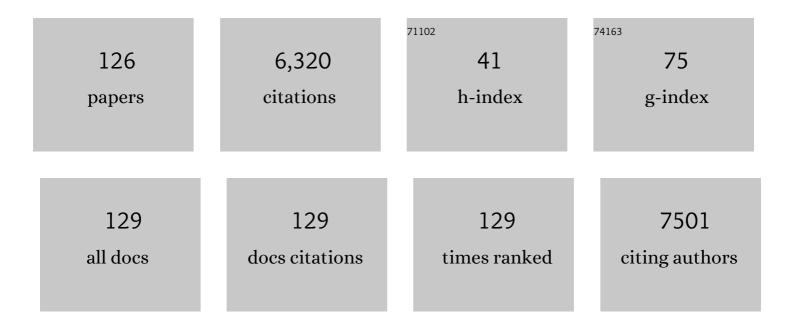
Jon Chorover

List of Publications by Year in descending order

Source: https://exaly.com/author-pdf/2153669/publications.pdf Version: 2024-02-01



#	Article	IF	CITATIONS
1	Analysis of hydrophilic per- and polyfluorinated sulfonates including trifluoromethanesulfonate using solid phase extraction and mixed-mode liquid chromatography-tandem mass spectrometry. Journal of Chromatography A, 2022, 1664, 462817.	3.7	6
2	Biosolids leachate variability, stabilization surrogates, and optical metric selection. Environmental Science: Water Research and Technology, 2022, 8, 657-670.	2.4	2
3	Fate of bis-(4-tert-butyl phenyl)-iodonium under photolithography relevant irradiation and the environmental risk properties of the formed photoproducts. Environmental Science and Pollution Research, 2022, 29, 25988-25994.	5.3	0
4	Resiliency of Silica Export Signatures When Low Order Streams Are Subject to Storm Events. Journal of Geophysical Research G: Biogeosciences, 2022, 127, .	3.0	6
5	Constraints of Climate and Age on Soil Development in Hawaiâ€~i. , 2022, , 49-88.		3
6	Enhanced removal of per- and polyfluoroalkyl substances by crosslinked polyaniline polymers. Chemical Engineering Journal, 2022, 446, 137246.	12.7	8
7	Metal Lability and Mass Transfer Response to Direct-Planting Phytostabilization of Pyritic Mine Tailings. Minerals (Basel, Switzerland), 2022, 12, 757.	2.0	2
8	Tailored Polyanilines Are High-Affinity Adsorbents for Per- and Polyfluoroalkyl Substances. ACS ES&T Water, 2022, 2, 1402-1410.	4.6	2
9	Effects of flow on uranium speciation in soils impacted by acidic waste fluids. Journal of Environmental Radioactivity, 2022, 251-252, 106955.	1.7	0
10	Experimental weathering of a volcaniclastic critical zone profile: Key role of colloidal constituents in aqueous geochemical response. Chemical Geology, 2021, 559, 119886.	3.3	3
11	Signatures of Hydrologic Function Across the Critical Zone Observatory Network. Water Resources Research, 2021, 57, e2019WR026635.	4.2	31
12	Bioconcentration potential and microbial toxicity of onium cations in photoacid generators. Environmental Science and Pollution Research, 2021, 28, 8915-8921.	5.3	7
13	Biochar-templated surface precipitation and inner-sphere complexation effectively removes arsenic from acid mine drainage. Environmental Science and Pollution Research, 2021, 28, 45519-45533.	5.3	10
14	Synthesis and Characterization of Customizable Polyaniline-Derived Polymers and Their Application for Perfluorooctanoic Acid Removal from Aqueous Solution. ACS ES&T Water, 2021, 1, 1438-1446.	4.6	3
15	U-series and Sr isotopes as tracers of mineral weathering and water routing from the deep Critical Zone to streamflow in a high-elevation volcanic catchment. Chemical Geology, 2021, 570, 120156.	3.3	5
16	Hydrogeophysical comparison of hillslope critical zone architecture for different geologic substrates. Geophysics, 2021, 86, WB87-WB107.	2.6	5
17	Photochemical fate of sulfonium photoacid generator cations under photolithography relevant UV irradiation. Journal of Photochemistry and Photobiology A: Chemistry, 2021, 416, 113324.	3.9	5
18	Phosphate controls uranium release from acidic waste-weathered Hanford sediments. Journal of Hazardous Materials, 2021, 416, 126240.	12.4	9

#	Article	IF	CITATIONS
19	Iron-activated persulfate oxidation degrades aqueous Perfluorooctanoic acid (PFOA) at ambient temperature. Chemosphere, 2021, 281, 130824.	8.2	19
20	Iron(II) monosulfide (FeS) minerals reductively transform the insensitive munitions compounds 2,4-dinitroanisole (DNAN) and 3-nitro-1,2,4-triazol-5-one (NTO). Chemosphere, 2021, 285, 131409.	8.2	10
21	Contrasting Community Assembly Forces Drive Microbial Structural and Potential Functional Responses to Precipitation in an Incipient Soil System. Frontiers in Microbiology, 2021, 12, 754698.	3.5	4
22	The Role of Manganese Dioxide in the Natural Formation of Organochlorines. ACS ES&T Water, 2021, 1, 2523-2530.	4.6	2
23	Resolving Deep Critical Zone Architecture in Complex Volcanic Terrain. Journal of Geophysical Research F: Earth Surface, 2020, 125, e2019JF005189.	2.8	13
24	Arsenic and iron speciation and mobilization during phytostabilization of pyritic mine tailings. Geochimica Et Cosmochimica Acta, 2020, 286, 306-323.	3.9	19
25	Dissolved Carbonate and pH Control the Dissolution of Uranyl Phosphate Minerals in Flow-Through Porous Media. Environmental Science & Technology, 2020, 54, 6031-6042.	10.0	11
26	Strong slopeâ€aspect control of regolith thickness by bedrock foliation. Earth Surface Processes and Landforms, 2020, 45, 2998-3010.	2.5	17
27	Effect of Re-acidification on Buffalo Grass Rhizosphere and Bulk Microbial Communities During Phytostabilization of Metalliferous Mine Tailings. Frontiers in Microbiology, 2019, 10, 1209.	3.5	24
28	Soil Fluid Biogeochemical Response to Climatic Events. Journal of Geophysical Research G: Biogeosciences, 2019, 124, 2866-2882.	3.0	8
29	Rare earth elements (REY) sorption on soils of contrasting mineralogy and texture. Environment International, 2019, 128, 279-291.	10.0	34
30	Microtopography-mediated hydrologic environment controls elemental migration and mineral weathering in subalpine surface soils of subtropical monsoonal China. Geoderma, 2019, 344, 82-98.	5.1	26
31	Assessing Microbial Community Patterns During Incipient Soil Formation From Basalt. Journal of Geophysical Research G: Biogeosciences, 2019, 124, 941-958.	3.0	16
32	Distinct stores and the routing of water in the deep critical zone of a snow-dominated volcanic catchment. Hydrology and Earth System Sciences, 2019, 23, 4661-4683.	4.9	17
33	Hydrologic functioning of the deep critical zone and contributions to streamflow in a highâ€elevation catchment: Testing of multiple conceptual models. Hydrological Processes, 2019, 33, 476-494.	2.6	22
34	Surficial weathering of kaolin regolith in a subtropical climate: Implications for supergene pedogenesis and bedrock argillization. Geoderma, 2019, 337, 225-237.	5.1	10
35	Oxidative Weathering Decreases Bioaccessibility of Toxic Metal(loid)s in PM ₁₀ Emissions From Sulfide Mine Tailings. GeoHealth, 2018, 2, 118-138.	4.0	19
36	Oxidation of reduced daughter products from 2,4-dinitroanisole (DNAN) by Mn(IV) and Fe(III) oxides. Chemosphere, 2018, 201, 790-798.	8.2	14

#	Article	IF	CITATIONS
37	Mechanisms of Arsenic Sequestration by <i>Prosopis juliflora</i> during the Phytostabilization of Metalliferous Mine Tailings. Environmental Science & Technology, 2018, 52, 1156-1164.	10.0	32
38	Uranium speciation in acid waste-weathered sediments: The role of aging and phosphate amendments. Applied Geochemistry, 2018, 89, 109-120.	3.0	17
39	Treatment impacts on temporal microbial community dynamics during phytostabilization of acid-generating mine tailings in semiarid regions. Science of the Total Environment, 2018, 618, 357-368.	8.0	32
40	Subsurface Pore Water Contributions to Stream Concentration-Discharge Relations Across a Snowmelt Hydrograph. Frontiers in Earth Science, 2018, 6, .	1.8	18
41	Abiotic reduction of insensitive munition compounds by sulfate green rust. Environmental Chemistry, 2018, 15, 259.	1.5	16
42	A considerable fraction of soil-respired CO2 is not emitted directly to the atmosphere. Scientific Reports, 2018, 8, 13518.	3.3	34
43	Adsorption and oxidation of 3-nitro-1,2,4-triazole-5-one (NTO) and its transformation product (3-amino-1,2,4-triazole-5-one, ATO) at ferrihydrite and birnessite surfaces. Environmental Pollution, 2018, 240, 200-208.	7.5	16
44	Wet–dry cycles impact DOM retention in subsurface soils. Biogeosciences, 2018, 15, 821-832.	3.3	14
45	Trapping of lead (Pb) by corn and pea root border cells. Plant and Soil, 2018, 430, 205-217.	3.7	14
46	CO ₂ diffusion into pore spaces limits weathering rate of an experimental basalt landscape. Geology, 2017, 45, 203-206.	4.4	13
47	Ecosystem Composition Controls the Fate of Rare Earth Elements during Incipient Soil Genesis. Scientific Reports, 2017, 7, 43208.	3.3	31
48	Bacterial Rhizoplane Colonization Patterns of Buchloe dactyloides Growing in Metalliferous Mine Tailings Reflect Plant Status and Biogeochemical Conditions. Microbial Ecology, 2017, 74, 853-867.	2.8	20
49	Geochemical evolution of the <scp>C</scp> ritical <scp>Z</scp> one across variable time scales informs concentrationâ€discharge relationships: <scp>J</scp> emez <scp>R</scp> iver <scp>B</scp> asin <scp>C</scp> ritical <scp>Z</scp> one <scp>O</scp> bservatory. Water Resources Research, 2017, 53, 4169-4196.	4.2	57
50	Rates and mechanisms of uranyl oxyhydroxide mineral dissolution. Geochimica Et Cosmochimica Acta, 2017, 207, 298-321.	3.9	12
51	Environmental Fate of ¹⁴ C Radiolabeled 2,4-Dinitroanisole in Soil Microcosms. Environmental Science & Technology, 2017, 51, 13327-13334.	10.0	13
52	Uranium Release from Acidic Weathered Hanford Sediments: Single-Pass Flow-Through and Column Experiments. Environmental Science & Technology, 2017, 51, 11011-11019.	10.0	15
53	Concentrationâ€Ðischarge Relations in the Critical Zone: Implications for Resolving Critical Zone Structure, Function, and Evolution. Water Resources Research, 2017, 53, 8654-8659.	4.2	48
54	Sequential anaerobic-aerobic biodegradation of emerging insensitive munitions compound 3-nitro-1,2,4-triazol-5-one (NTO). Chemosphere, 2017, 167, 478-484.	8.2	38

#	Article	IF	CITATIONS
55	Designing a network of critical zone observatories to explore the living skin of the terrestrial Earth. Earth Surface Dynamics, 2017, 5, 841-860.	2.4	92
56	Identifying Toxic Biotransformation Products of the Insensitive Munitions Compound, 2,4-Dinitroanisole (DNAN), Using Liquid Chromatography Coupled to Quadrupole Time-of-Flight Mass Spectrometry (LC-QToF-MS). ACS Symposium Series, 2016, , 133-145.	0.5	2
57	Pore water chemistry reveals gradients in mineral transformation across a model basaltic hillslope. Geochemistry, Geophysics, Geosystems, 2016, 17, 2054-2069.	2.5	11
58	Phytostabilization of mine tailings using compost-assisted direct planting: Translating greenhouse results to the field. Science of the Total Environment, 2016, 565, 451-461.	8.0	102
59	Microbial toxicity and characterization of DNAN (bio)transformation product mixtures. Chemosphere, 2016, 154, 499-506.	8.2	16
60	U-series isotopic signatures of soils and headwater streams in a semi-arid complex volcanic terrain. Chemical Geology, 2016, 445, 68-83.	3.3	13
61	Colloids and organic matter complexation control trace metal concentration-discharge relationships in Marshall Gulch stream waters. Water Resources Research, 2016, 52, 7931-7944.	4.2	45
62	Resolving colocalization of bacteria and metal(loid)s on plant root surfaces by combining fluorescence in situ hybridization (FISH) with multiple-energy micro-focused X-ray fluorescence (ME) Tj ETQq0	0 0 r g.B T /O	verbock 10 Tf
63	Soil Lysimeter Excavation for Coupled Hydrological, Geochemical, and Microbiological Investigations. Journal of Visualized Experiments, 2016, , .	0.3	4
64	(Bio)transformation of 2,4-dinitroanisole (DNAN) in soils. Journal of Hazardous Materials, 2016, 304, 214-221.	12.4	46
65	Solid-phase redistribution of rare earth elements in hillslope pedons subjected to different hydrologic fluxes. Chemical Geology, 2016, 426, 1-18.	3.3	23
66	Climatic and landscape controls on water transit times and silicate mineral weathering in the critical zone. Water Resources Research, 2015, 51, 6036-6051.	4.2	43
67	Adsorption of novel insensitive munitions compounds at clay mineral and metal oxide surfaces. Environmental Chemistry, 2015, 12, 74.	1.5	38
68	Critical Zone Services: Expanding Context, Constraints, and Currency beyond Ecosystem Services. Vadose Zone Journal, 2015, 14, vzj2014.10.0142.	2.2	60
69	Hydrological partitioning in the critical zone: Recent advances and opportunities for developing transferable understanding of water cycle dynamics. Water Resources Research, 2015, 51, 6973-6987.	4.2	189
70	Quantifying Topographic and Vegetation Effects on the Transfer of Energy and Mass to the Critical Zone. Vadose Zone Journal, 2015, 14, 1-16.	2.2	37
71	The Landscape Evolution Observatory: A large-scale controllable infrastructure to study coupled Earth-surface processes. Geomorphology, 2015, 244, 190-203.	2.6	47
72	Toxic metal(loid) speciation during weathering of iron sulfide mine tailings under semi-arid climate. Applied Geochemistry, 2015, 62, 131-149.	3.0	65

#	Article	IF	CITATIONS
73	The Role of Critical Zone Observatories in Critical Zone Science. Developments in Earth Surface Processes, 2015, , 15-78.	2.8	57
74	Biotransformation and Degradation of the Insensitive Munitions Compound, 3-Nitro-1,2,4-triazol-5-one, by Soil Bacterial Communities. Environmental Science & Technology, 2015, 49, 5681-5688.	10.0	54
75	Rare earth elements as reactive tracers of biogeochemical weathering in forested rhyolitic terrain. Chemical Geology, 2015, 391, 19-32.	3.3	67
76	Experimental Assessment of Passive Capillary Wick Sampler Suitability for Inorganic Soil Solution Constituents. Soil Science Society of America Journal, 2014, 78, 486-495.	2.2	7
77	Incipient subsurface heterogeneity and its effect on overland flow generation – insight from a modeling study of the first experiment at the Biosphere 2 Landscape Evolution Observatory. Hydrology and Earth System Sciences, 2014, 18, 1873-1883.	4.9	29
78	Hillslope-scale experiment demonstrates the role of convergence during two-step saturation. Hydrology and Earth System Sciences, 2014, 18, 3681-3692.	4.9	31
79	Fractionation of Dissolved Organic Matter by (Oxy)Hydroxideâ€Coated Sands: Competitive Sorbate Displacement during Reactive Transport. Vadose Zone Journal, 2014, 13, 1-13.	2.2	22
80	Bioaccessibility, release kinetics, and molecular speciation of arsenic and lead in geo-dusts from the Iron King Mine Federal Superfund site in Humboldt, Arizona. Reviews on Environmental Health, 2014, 29, 23-7.	2.4	8
81	Stream water carbon controls in seasonally snow-covered mountain catchments: impact of inter-annual variability of water fluxes, catchment aspect and seasonal processes. Biogeochemistry, 2014, 118, 273-290.	3.5	60
82	Influence of Phosphate and Silica on U(VI) Precipitation from Acidic and Neutralized Wastewaters. Environmental Science & Technology, 2014, 48, 6097-6106.	10.0	59
83	Environmental factors influencing the structural dynamics of soil microbial communities during assisted phytostabilization of acid-generating mine tailings: A mesocosm experiment. Science of the Total Environment, 2014, 500-501, 314-324.	8.0	67
84	Surficial weathering of iron sulfide mine tailings under semi-arid climate. Geochimica Et Cosmochimica Acta, 2014, 141, 240-257.	3.9	79
85	Impact of organic carbon on weathering and chemical denudation of granular basalt. Geochimica Et Cosmochimica Acta, 2014, 139, 508-526.	3.9	19
86	A New Standard-Based Polynomial Interpolation (SBPIn) method to address gel-to-gel variability for the comparison of multiple denaturing gradient gel electrophoresis profile matrices. Journal of Microbiological Methods, 2013, 92, 173-177.	1.6	5
87	Fractionation of yttrium and holmium during basaltic soil weathering. Geochimica Et Cosmochimica Acta, 2013, 119, 18-30.	3.9	37
88	Effect of silicic acid on arsenate and arsenite retention mechanisms on 6-L ferrihydrite: A spectroscopic and batch adsorption approach. Applied Geochemistry, 2013, 38, 110-120.	3.0	84
89	Microscale Speciation of Arsenic and Iron in Ferric-Based Sorbents Subjected to Simulated Landfill Conditions. Environmental Science & Technology, 2013, 47, 12992-13000.	10.0	32
90	Coevolution of nonlinear trends in vegetation, soils, and topography with elevation and slope aspect: A case study in the sky islands of southern Arizona. Journal of Geophysical Research F: Earth Surface, 2013, 118, 741-758.	2.8	76

#	Article	IF	CITATIONS
91	Impacts of Sampling Dissolved Organic Matter with Passive Capillary Wicks Versus Aqueous Soil Extraction. Soil Science Society of America Journal, 2012, 76, 2019-2030.	2.2	16
92	Adsorption of perfluorooctanoic acid and perfluorooctanesulfonic acid to iron oxide surfaces as studied by flow-through ATR-FTIR spectroscopy. Environmental Chemistry, 2012, 9, 148.	1.5	156
93	Geochemical Weathering Increases Lead Bioaccessibility in Semi-Arid Mine Tailings. Environmental Science & Technology, 2012, 46, 5834-5841.	10.0	48
94	Quantifying PPCP interaction with dissolved organic matter in aqueous solution: Combined use of fluorescence quenching and tandem mass spectrometry. Water Research, 2012, 46, 943-954.	11.3	83
95	Response of Key Soil Parameters during Compost-Assisted Phytostabilization in Extremely Acidic Tailings: Effect of Plant Species. Environmental Science & Technology, 2012, 46, 1019-1027.	10.0	73
96	Changes in Zinc Speciation with Mine Tailings Acidification in a Semiarid Weathering Environment. Environmental Science & Technology, 2011, 45, 7166-7172.	10.0	19
97	The effects of climate and landscape position on chemical denudation and mineral transformation in the Santa Catalina mountain critical zone observatory. Applied Geochemistry, 2011, 26, S80-S84.	3.0	19
98	A mass-balance model to separate and quantify colloidal and solute redistributions in soil. Chemical Geology, 2011, 282, 113-119.	3.3	34
99	Interactions of Carbamazepine in Soil: Effects of Dissolved Organic Matter. Journal of Environmental Quality, 2011, 40, 942-948.	2.0	75
100	Trace contaminant concentration affects mineral transformation and pollutant fate in hydroxide-weathered Hanford sediments. Journal of Hazardous Materials, 2011, 197, 119-127.	12.4	21
101	Effect of arbuscular mycorrhizal fungi on plant biomass and the rhizosphere microbial community structure of mesquite grown in acidic lead/zinc mine tailings. Science of the Total Environment, 2011, 409, 1009-1016.	8.0	100
102	An open system framework for integrating critical zone structure and function. Biogeochemistry, 2011, 102, 15-29.	3.5	103
103	How Water, Carbon, and Energy Drive Critical Zone Evolution: The Jemez–Santa Catalina Critical Zone Observatory. Vadose Zone Journal, 2011, 10, 884-899.	2.2	111
104	Rare earth element release from phosphate minerals in the presence of organic acids. Chemical Geology, 2010, 278, 1-14.	3.3	96
105	Changes in lead and zinc lability during weathering-induced acidification of desert mine tailings: Coupling chemical and micro-scale analyses. Applied Geochemistry, 2009, 24, 2234-2245.	3.0	42
106	Solid phase evolution in the Biosphere 2 hillslope experiment as predicted by modeling of hydrologic and geochemical fluxes. Hydrology and Earth System Sciences, 2009, 13, 2273-2286.	4.9	23
107	ATR-FTIR study of lipopolysaccharides at mineral surfaces. Colloids and Surfaces B: Biointerfaces, 2008, 62, 188-198.	5.0	42
108	Soil Biogeochemical Processes within the Critical Zone. Elements, 2007, 3, 321-326.	0.5	224

#	Article	IF	CITATIONS
109	ATR-FTIR Spectroscopy Reveals Bond Formation During Bacterial Adhesion to Iron Oxide. Langmuir, 2006, 22, 8492-8500.	3.5	307
110	Colloid Mobilization During Soil Iron Redox Oscillations. Environmental Science & Technology, 2006, 40, 5743-5749.	10.0	163
111	Linking litter calcium, earthworms and soil properties: a common garden test with 14 tree species. Ecology Letters, 2005, 8, 811-818.	6.4	586
112	Surface charge evolution of mineral-organic complexes during pedogenesis in Hawaiian basalt. Geochimica Et Cosmochimica Acta, 2004, 68, 4859-4876.	3.9	187
113	Reaction of forest floor organic matter at goethite, birnessite and smectite surfaces. Geochimica Et Cosmochimica Acta, 2001, 65, 95-109.	3.9	309
114	The chemistry of pedogenic thresholds. Geoderma, 2001, 100, 321-353.	5.1	358
115	Leachate Chemistry of Fieldâ€Weathered Spent Mushroom Substrate. Journal of Environmental Quality, 2001, 30, 1699-1709.	2.0	43
116	Effects of Spent Mushroom Substrate Weathering on the Chemistry of Underlying Soils. Journal of Environmental Quality, 2001, 30, 2127-2134.	2.0	19
117	Response to "Comments on â€~Artifacts Caused by Collection of Soil Solution with Passive Capillary Samplers'― Soil Science Society of America Journal, 2001, 65, 1572-1573.	2.2	3
118	Rapid abiotic transformation of nitrate in an acid forest soil. Biogeochemistry, 2001, 54, 131-146.	3.5	157
119	Evolution of CO ₂ during Birnessiteâ€Induced Oxidation of ¹⁴ Câ€Labeled Catechol. Soil Science Society of America Journal, 2000, 64, 157-163.	2.2	58
120	Artifacts Caused by Collection of Soil Solution with Passive Capillary Samplers. Soil Science Society of America Journal, 2000, 64, 1330-1336.	2.2	35
121	Structural Charge and Cesium Retention in a Chronosequence of Tephritic Soils. Soil Science Society of America Journal, 1999, 63, 169-177.	2.2	45
122	Quinoline Sorption on Kaolinite–Humic Acid Complexes. Soil Science Society of America Journal, 1999, 63, 850-857.	2.2	37
123	Surface charge characteristics of kaolinitic tropical soils. Geochimica Et Cosmochimica Acta, 1995, 59, 875-884.	3.9	122
124	Colloid Chemistry of Kaolinitic Tropical Soils. Soil Science Society of America Journal, 1995, 59, 1558-1564.	2.2	30
125	Solution chemistry profiles of mixed-conifer forests before and after fire. Biogeochemistry, 1994, 26, 115-144.	3.5	97
126	Controlled Experiments of Hillslope Coevolution at the Biosphere 2 Landscape Evolution Observatory: Toward Prediction of Coupled Hydrological, Biogeochemical, and Ecological Change. , 0,		9